Supplementary Material

Low-RCS Coding Metasurface Utilizing 3-D Printed ABS Shells and Carbonyl Iron Powder/Polyimide Composite Patches via Hybrid Mechanisms

Sen Zhang [a]; Qing An [b]; Dawei Li [b,c]; Ke Chen[a]; Junming Zhao [a,*]; Tian Jiang [a,*]; Wenhe Liao [b,c]; Tingting Liu [b]; Yijun Feng [a]

[a] School of Electronic Science and Engineering, Nanjing University, Nanjing, 210023, China

[b] School of Mechanical Engineering (SME), Nanjing University of Science and Technology, 200 Xiao Ling Wei Road, Nanjing, 210094, China

[c] School of Mechanical Engineering, Key Laboratory of Special Engine Technology, Ministry of Education, Nanjing University of Science and Technology, Nanjing, Jiangsu 210094, China

* Corresponding author.
Email: jmzhao@nju.edu.cn (J. Zhao), jt@nju.edu.cn (T. Jiang)

Section S1. Characterization of the self-made CIP/PI composite

The electromagnetic (EM) parameters of the CIP/PI composite are characterized using the coaxial-line method via a vector network analyzer (Agilent N5244). As shown in **Fig. S1(a)**, both its permittivity and permeability have a relatively large loss tangent, indicating excellent EM loss characteristics. The microscopic morphological image of carbonyl iron powder/polyimide (CIP/PI) composite patch which is obtained by a SEM (Crossbeam 350) is shown in **Fig. S1(b)**. We can find from **Fig. S1(b)** that carbonyl iron powder (CIP) is uniformly dispersed in their based materials (PI). Therefore, the CIP/PI composite can interact with the incident EM waves stably.

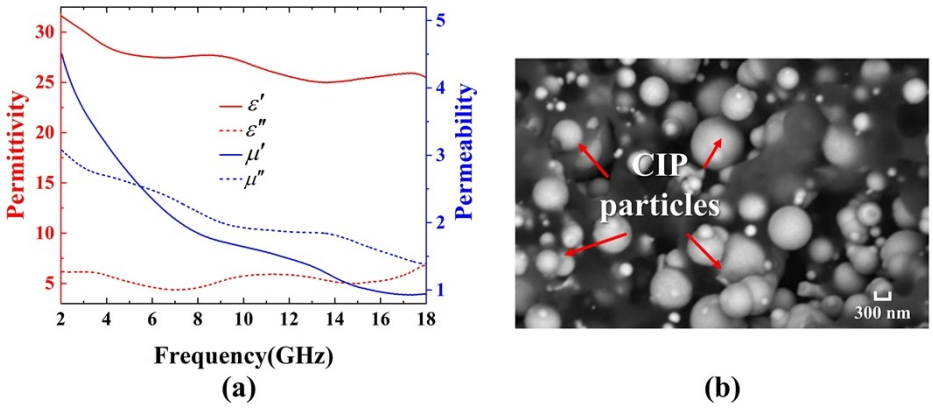

Fig. S1. (a) EM parameters and (b) SEM images of the CIP/PI composite.

Section S2. Detailed parameter research for unit cells based on ABS shells and planar CIP/PI composite patches

The detailed parameter research process of the unit cells in Metasurface 1 is as follows. The impact of the air layer height t_a within the ABS shell on reflection is illustrated in **Fig. S2**. It is evident that t_a has a minimal impact on low-frequency absorption performance but significantly influences the reflection magnitude near 10 GHz and the reflection phase at 18 GHz. However, **Fig. S3** demonstrates that variations in the CIP/PI composite patch thickness t_m directly influence the reflection magnitude and phase at low frequencies. Furthermore, variations in the thickness t_h of the ABS shell significantly influence the overall reflection magnitude and have a notable impact on the reflection phase at high frequencies which is shown in **Fig. S4**.

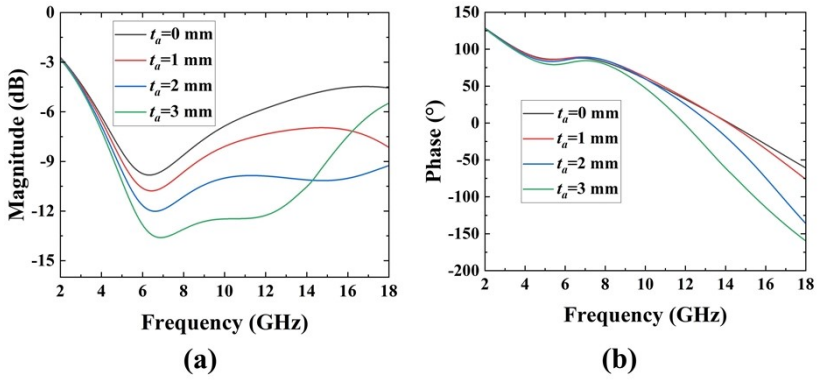

Fig. S2. Reflection magnitude (a) and phase (b) under different t_a when t_m is 1 and t_h is 1.

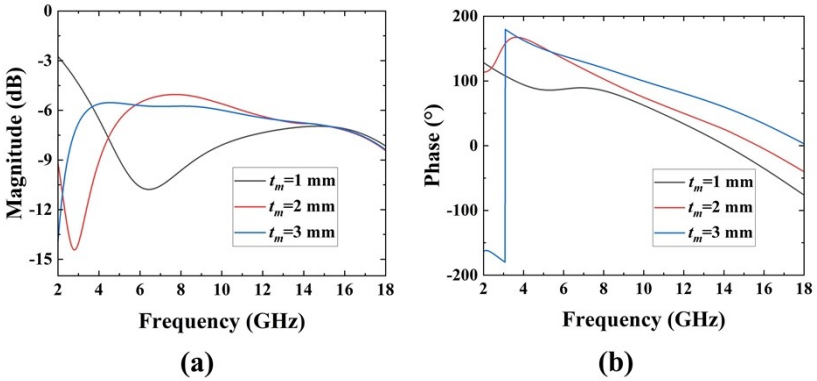

Fig. S3. Reflection magnitude (a) and phase (b) under different t_m when t_a is 1 and t_h is 1.

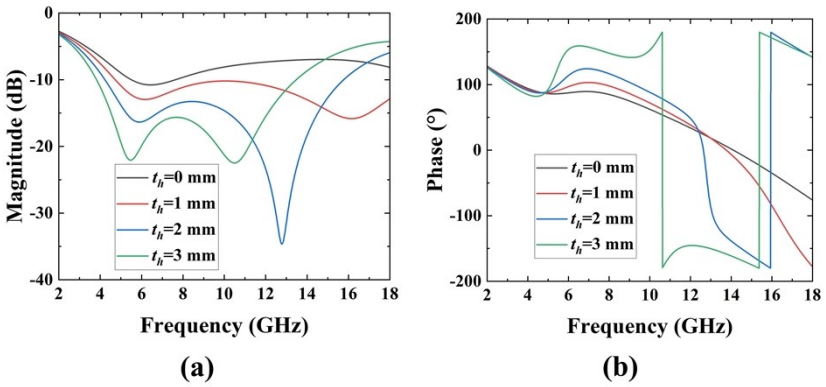

Fig. S4. Reflection magnitude (a) and phase (b) under different t_h when t_a is 1 and t_m is 1.

Section S3. Parameter settings and procedures for genetic algorithms (GA)

We can see the flowchart of GA in the case of array optimization from **Fig. S5(a)**. In the case of array optimization, we take each coding matrix which represents a type of unit cell arrangements as an individual. First, we generate 30 codes to initialize the population. The fitness for each encoding is then calculated. In the selection process, we first randomly selected two individuals, and then selected the one with the greater fitness for crossover. We discretize the 2–18GHz spectrum into 441 frequencies to calculate the RCS reduction. Therefore, the value of Q is 440. If the RCS reduction at a frequency is more than 10 dB, then the value of fitness at that frequency is 1. The detailed crossover process is shown in **Fig S5(b)**. We change the 4×4 coding matrix to a 1×16 matrix. For the selected individuals A and B, the elements are randomly selected to combine into a new individual. All elements of the new individual mutate into other elements with a 1.5% chance. The maximum number of iterations G is set to 100.

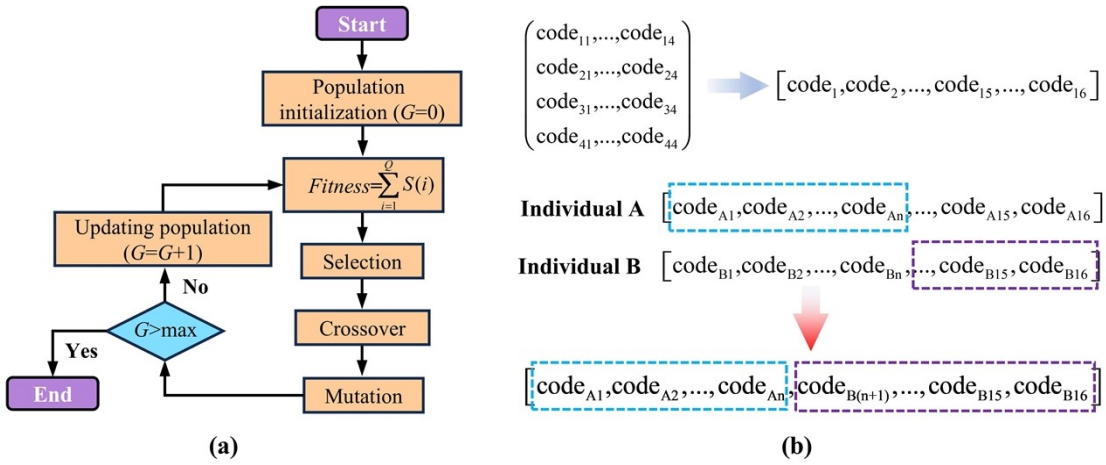

Fig. S5. (a) Flowchart of GA in the case of array optimization. (b) Detailed crossover process.

Section S4. Detailed parameter research for unit cells based on ABS shells and stepped CIP/PI composite patches

The detailed parameter study of the unit cells in Metasurface 2 is described as follows. As shown in **Fig. S6**, the thickness t_h of the ABS shell primarily influences the absorption performance at high frequencies and significantly affects the reflection phase at these frequencies. As illustrated in **Fig. S7**, increasing the side length P_1 of the top CIP/PI composite patch results in a shift of the lowest frequency absorption peak towards lower frequencies. **Fig. S8** indicates that variations in the air layer height t_a primarily affect high-frequency EM waves, with minimal influence on lower frequencies.

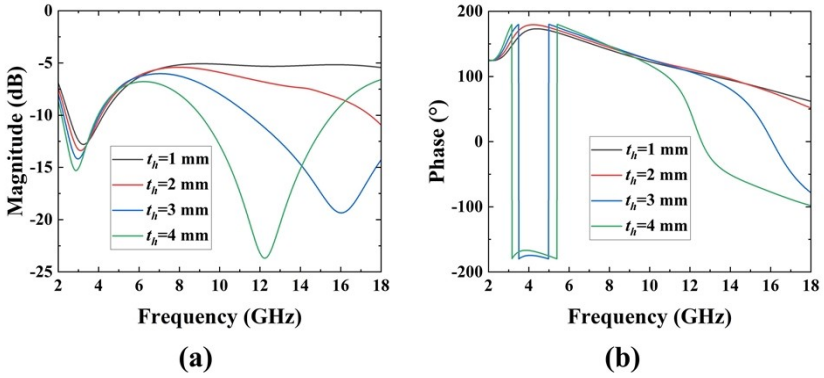

Fig. S6. Reflection magnitude (a) and phase (b) under different t_h when t_{m1}, t_{m2} and t_a are all 1 and P_1 is 18.

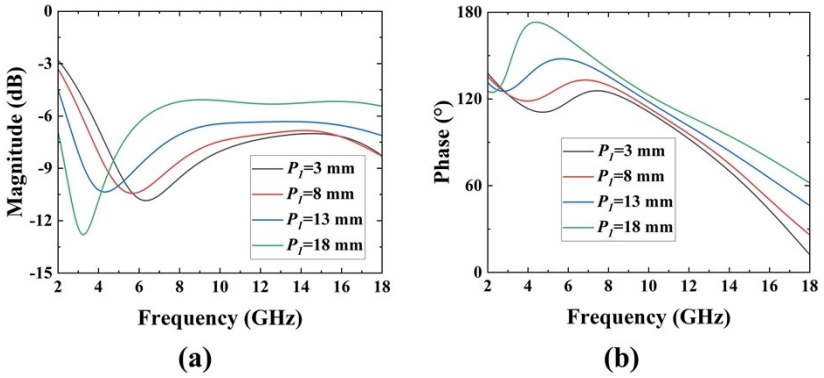

Fig. S7. Reflection magnitude (a) and phase (b) under different P_1 when t_{m1}, t_{m2}, t_a and t_h are all 1.

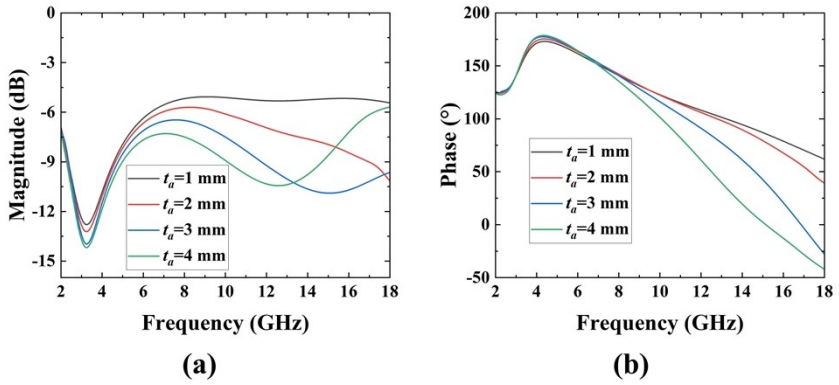

Fig. S8. Reflection magnitude (a) and phase (b) under different t_a when t_{m1}, t_{m2} and t_h are all 1 and P_1 is 18.

Section S5. RCS reduction performance of Metasurface 2 at oblique incidence

From **Fig. S9(a)**, it can be observed that under TE polarization, the RCS reduction performance of the metasurface begins to deteriorate as the oblique incidence angle increases. However, even at an oblique incidence angle of 45°, the RCS reduction remains greater than 6 dB across the frequency range of 2-18 GHz. **Fig. 9(b)** indicates that the RCS reduction performance of the metasurface under TM polarization actually improves as the incident angle increases.

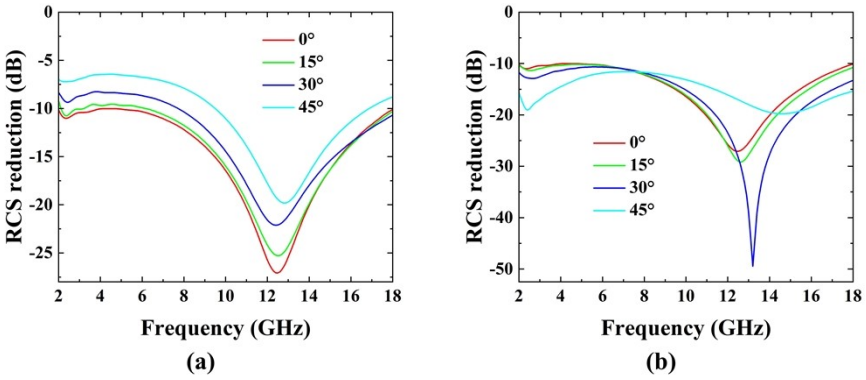

Fig. S9. RCS reduction of Metasurface 2 under (a) TE and (b) TM polarization at oblique incidence.